Characterization of Intestinal Permeability using 2D and 3D Mouse Intestinal Organoids

Initially thought to mainly play a role in gut pathologies such as Inflammatory Bowel Disease (IBD), the gut microbiome has recently been linked with a variety of neurodegenerative disease through the Gut-Microbiome-Brain axis. This emerging bidirectional link between the gut, the microbiome that inhabits it and the CNS has been implicated in diseases like Multiple Sclerosis and Alzheimer's disease through a growing body of evidence. Patients suffering from these illnesses have been shown to have altered microbiome composition, gut dysbiosis and an increasingly permeable gut. Furthermore, studies of immunodeficient mice, such as AICDA -/- mice have shown that the lack of IgA producing plasma cells can lead to dysbiosis and gut permeability like that observed in patients suffering from neurodegeneration. To study these interactions in a controlled and reproducible environment, this study aims to produce and characterize 2D and 3D Mouse Intestinal Organoid that mimic in-vivo gut barrier function and allow for the co-culture with immune cells and gut flora.

Introduction

Organization of the Intestinal Epithelium

The intestinal epithelium is a specialized single cell thick layer essential for segregation and mediation in the gut environment. It can be divided into several distinct regions (Figure 1). The apical side consists of the lumen and houses your microbiome/commensals as well as a layer of mucus. The basolateral side consists of the lamina propria, a layer of connective tissue containing lymphoid cells/structures, as well as a variety of muscle tissue and enteric nerves. Lastly, the cell layer itself consists of a variety of cells all carrying out separate essential functions[1]. The cell layer of the intestinal epithelium is arranged in villi as a means of maximizing surface area, this is visualized as alternating peaks and dips (Figure 1). The "dips" in the structure of the villi are formally termed "Crypts of Lieberkühn" or "Crypts" and contain immature undifferentiated stem cells[1]. The differentiation and expansion of these stem cells results in the steady regeneration of the intestinal epithelium. The crypts are also the predominant location for Paneth cells which are secretory cells responsible for producing antimicrobial peptides (AMPs). The production of these AMPs helps in modulating the size and composition of the microbiome to a level that won't confer harm to the body[2]. Other important cells include goblet cells which produce the mucosal layer which acts as a physical barrier as well as enteroendocrine cells responsible for hormone signaling[2].

All regions work together to maintain homeostasis in the gut as well as in other connected areas in the body, however, their segregation is an essential component of their function. The intestinal epithelium is said to be polarized, meaning the apical and basolateral facing sides of the cell layer express distinct markers and carry out different functions[3-4]. This polarity is maintained by junction proteins which work to separate the basolateral and apical sections of the membrane[3-4]. Some of these junction proteins, which are vital for barrier function are known as tight junction proteins and include proteins like ZO1 and Occludin[3-4]. Studies of Occludin knockout mice have shown that slower forming and less stable tight junctions contribute to chronic inflammation and hyperplasia in gut tissue[5]. Similarly, studies have shown that ZO1 deficient cells exhibited slower tight junction formation and that tight junction disruption predisposes mice to Inflammatory Bowel Disease[6]. Therefore, the maintenance of this polarization is vital for proper function of the intestinal epithelium and loss of polarization can lead to increased gut permeability and risk of pathologies.

The Intestinal epithelium and Microbiome

The gut microbiome consists of the collective genomes of various microbes such as bacteria, archaea and protozoa that inhabit your gut. In healthy individuals, these are described as commensals meaning they confer little harm and varying levels of benefits[7]. The lumen of the intestinal epithelium acts as the primary interface between this gut microbiome and the body. Here, a delicate balance exists where the gut environment simultaneously provides nutrients and room for growth for the commensals while regulating the population using AMPs and other molecules[2]. This chemical barrier exists along with the physical barrier of mucus produced prevent bacterial infiltration into the lamina propria. However, there are some benefits of the interaction between the microbiome, microbial molecules, and cells in the lamina propria. The passage of these molecules is mediated by the epithelial cells as well specialized cells such as M cells. The exposure of your immune cells to these microbial antigens helps in the development of

tolerance which can be a factor in preventing autoimmune disease while also priming of your immune system against potential pathogens[8]. Abnormally increased populations of organisms producing these proinflammatory antigens can lead to chronic gut inflammation which is seen in illnesses like colitis[9-10]. On the other hand, too little exposure to the same antigens is associated with defects in the intestinal lymphoid tissue and function, such as deficiencies in IgA[11]. Researchers have also been able to draw causal links through the use of fecal transplants from donor mice with inflammatory bowel disease (IBD) to healthy mice which resulted in the onset of colitis through an altered immune response[12]. The complexity observed in the gut microbiome exemplifies the fragility of the balance that must be maintained and highlights how something as simple as the food we consume, can lead to gut dysbiosis.

Figure 1

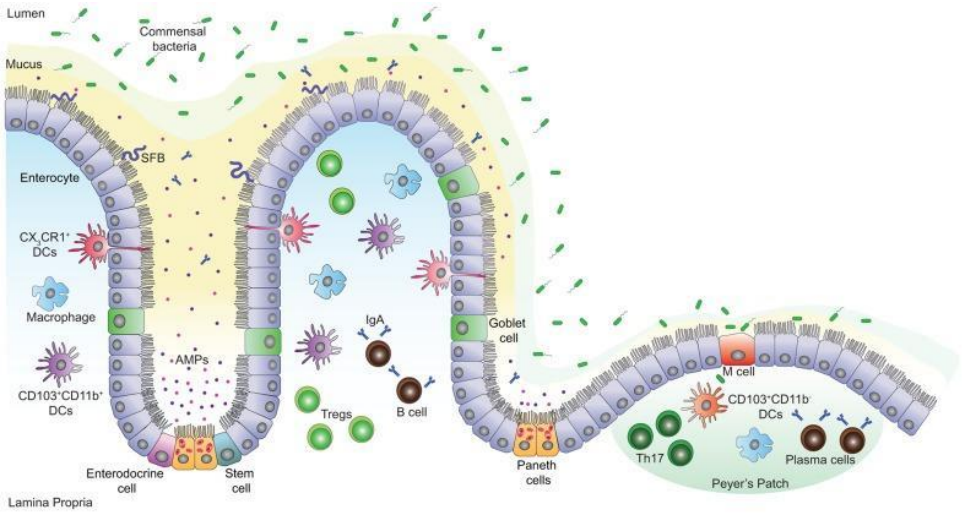

Figure 1: Structure of intestinal epithelium.

Gut-Microbiome-Brain Axis

The Gut-Microbiome-Brain Axis is the interconnected network of multidirectional communication and signaling between the gut, the microbiota that inhabit it and the Central Nervous system (CNS). This arises through a multitude of signaling pathways both directly and indirectly and is important for health and homeostasis[13]. One important mediator of this communication is the polarized intestinal epithelium. Through the onset of disease, this polarized barrier can become leaky and permeable to various microbial molecules which can prime the immune system for autoimmune inflammation and has been implicated in a variety of neurodegenerative disease[13]. So, while disruptions in the gut microbiome were initially linked with gut pathologies, the emerging links between the microbiome and the CNS have also been implicated in other diseases.

Multiple sclerosis is one such illness where the causality between alterations in the gut microbiome and neuroinflammation has been identified. Researchers have been able to identify specific organisms that are altered in MS and appear to be contributors to increased inflammation and autoimmunity. One example is the archaeon Methanobrevibacter which has been implicated

in inflammation through its ability recruit inflammatory cells and activate human dendritic cells[14]. Alternative studies have also demonstrated that patients suffering from relapsing-remitting MS (RRMS) have a distinct gut microbiome compared to healthy individuals and once again, researchers were able to pinpoint specific organisms that are either decreased or increased in RRMS[15]. Further investigation of how the varied microbiome composition impacted patients revealed that the gut microbiota of diseased individuals created a "sustained proinflammatory environment." When taken in conjunction with genetic and environmental risk factors, this sustained inflammation was identified as contributor to the autoimmune destruction of myelin[16]. For example, the organism *A. calcoaceticus* has been shown to produce antigens mimicking myelin basic protein (MBP) and MOG, two vital components of myelin[16]. This could potentially serve as one of the many mechanisms by which the gut microbiota causes autoimmunity. Ultimately, researchers have been able to show a direct causal link between the gut microbiome and MS using fecal transplants. These studies showed that transplants from donors with MS triggered EAE more frequently than transplants from healthy controls into germ free mice[17].

Role of IgA in Gut Homeostasis

Studies looking into risk factors into development of gut dysbiosis have identified mucosal IgA antibodies as a critical component in the regulation of bacterial composition. In studies of AICDA -/- mice (IgA deficient) researchers have shown that IgAs are a central element of the immune systems regulation of gut flora homeostasis[8,18-20]. IgMs on the other hand, although still secreted in the gut of AICDA -/- mice, could not prevent changes in the composition of the microbiome caused by the expansion of anaerobic population[20]. These primarily consisted of Segmented filamentous bacteria (SFBs) [20]. Other processes meant for microbiome composition control such as AMPs from Paneth cells also failed to produce effective response against the expansion of anaerobes. Only upon the reintroduction of IgA into the gut of AICDA -/- mice did the aberrant expansion of SFBs become regulated[20]. This evidence signifies an essential and unifying role of IgA in maintenance of gut homeostasis and contributed to the selection of AICDA -/- as models of disease in this project.

Organoids

Organoids are multicellular in-vitro 3D reconstructions that mimic the 3D structure, spatial arrangement, and cellular diversity of organs. Organoids allow for the study of organ tissues and organ environments without the need for an in-vivo organism while also preserving more tissue specific characteristics than standard 2D cell lines[21-22].

Mouse small intestinal 2D/3D Organoids

Mouse small intestinal 3D Organoids were first introduced in 2009 and have contributed to a paradigm shift in how intestinal permeability and gut dysbiosis are studied[23]. These organoids are derived from stem cells (ASCs or PSCs) and allow for the focused study of the intestinal epithelium ex-vivo while replicating the 3D spatial environment, molecular and cellular diversity of the in-vivo gut. Because 3D organoids can be leveraged ex-vivo, they are extremely potent to changes such as environmental or genetic manipulation making them a versatile model[24]. They are also cheaper to maintain and easier to observe than live mice while allowing for high throughput testing of molecules and experimental parameters. However, 3D organoids do come with their own drawbacks such, longevity, access to the lumen and lack of complex secondary environments such as immune interactions[24,25]. Some of these issues can be remedied using 2D

mouse monolayer organoids which preserve the cellular diversity while providing more freedom to alter the environment of the organoid. 2D Monolayer organoids should not be confused with 2D plated cell lines which often don't contain any cellular diversity or local specialization. 2D organoids can be accessed and observed from both the apical and basolateral sides allowing for easier collection and introduction of various molecules and cells (i.e. immune cells) to the environment surrounding the gut epithelium[22,25]. Because of their cost effectiveness, ease of use and versatility, 2D mouse monolayer organoids are an efficient model for the intestinal epithelium.

Research Aims

Aim 1: To assess changes in gut permeability in ex-vivo gut tissue from AICDA -/- Vs WT mice

The initial aim of the research project was to establish the presence of gut dysbiosis in AID knockout (AICDA -/-) mice. This was demonstrated previously by Shulzhenko et al[8] in the context of plasma cells and IgA production, however, is yet to be comprehensively explored through the lens of gut permeability and junction markers. To establish gut dysbiosis, multiple experiments were carried out to differentiate the gut permeability of wild type (WT) vs the AICDA -/-. These included the comparative immunofluorescence and RT-PCR of AICDA -/- vs WT mouse intestinal tissue for junction markers Occludin and E-Cadherin, as well serum ELISAs of gut permeability marker FABP2[26].

Aim 2. To generate an expandable 2D/3D mouse intestinal organoid lineage that could be used to study the previously established gut dysbiosis in a controlled environment

The secondary aim was the generation of. This would allow for a more focused breakdown of the exact mechanism by which AID/Plasma cell deficiency affects the gut permeability. To validate the organoids as a model, their barrier function was compared to that of the previous Wild Type mouse intestinal tissue. Once complete, the organoids were also to be tested as models of not only healthy mice, but diseased mice as well. The barrier function of intestinal tissue in AID knockout mice, would be assessed against the organoids and Wild type Tissue as a means of identifying differences and similarities in gut permeability.

Aim 3. Implement organoids as a model for studying the effects of specific bacterial cultures on immune cell phenotypes

The final research aim, which remains in progress, is the implementation of the organoids as a means of modelling interactions between monocultures and cocultures of bacteria with a variety of immune cells at the intestinal epithelium. This may shed light on specific phenotypic changes induced by bacteria that may influence the immune system's role in gut permeability and neurodegeneration.

Methods

Mice description

The wild type mice used in this study were C57BL/6 mice. The AICDA -/- mice used had a knockout of the AID gene which is responsible for the generation of highly specific antibody clonotypes in Germinal Centers through cross switch recombination and somatic hypermutation[27]. AICDA -/- mice are deficient in plasma cells.

Organoid Generation

Intestinal segments were rinsed with cold PBS and cut intestinal tissue into 2mm pieces. Intestinal pieces were placed in 50mL of PBS in a conical tube and pipetted up and down three times before being allowed to settle. Washing with PBS and pipetting steps were repeated until supernatant is clear. The supernatant was removed, and the tissue suspended in room temperature gentle dissociation reagent for 15min on a rocking platform. Tissue was left to settle, and supernatant was pipetted away. Cells were resuspended in cold PBS with 0.1% BSA. The supernatant was pipetted away and the solution was filtered. The tissue was centrifuged at 290g for 5 mins at 5C and subsequently the supernatant was discarded. Tissue pellets were resuspended in 10mL cold PBS with 0.1% BSA. Crypts were centrifuged at 200g for 3 mins at 5C and the supernatant was poured away. The crypts were resuspended in 10mL cold DMEM and aliquot sample into a desirable amount of crypts/volume. 150 µL of room temp IntestiCult™ Organoid Growth Medium (OGM) was added to pellets in each tube followed by 150 µL undiluted Matrigel® Matrix of undiluted matrigel matrix. The entire solution was resuspended. 50 µL of suspended samples is aliquoted into each well to form matrigel domes and the entire plate was placed at 37°C for 10 minutes to set the Matrigel. 750 µL room temp organoid growth medium was added to each well by pipetting down the side of the well, not directly on matrigel. Cultures were covered and incubated at 37°C and 5% CO2 with the culture medium being replaced three times per week/ Organoids were passaged every 7-10 days at a 1:2/1:3 ratio.

3D Organoid Fixation & Cryosectioning

OGM medium was removed without disturbing the basement membrane matrix and wells were gently washed once with 500 µL of PBS. Organoids were fixed with 1.0 mL of 4% paraformaldehyde (PFA) solution at RT for 30 min. The PFA solution was removed and each well was gently washed twice with 1 mL PBS. The PBS was removed and replaced with 1.0 mL of 30% sucrose buffer. Fixed organoids in sucrose were incubated for 1 h at 4 °C. The sucrose buffer was removed, and enough OCT was added directly to the well to cover the matrix layer. The organoids were incubated at Rt for 5 minutes followed by snap freezing on dry ice or by placing them in a −80 °C freezer. Once the embedding compound turns solid and white throughout, the dish was removed from the −80 °C freezer/dry ice and allowed to minimally melt. Friction was applied along the edge of each well with forceps to accelerate the melting of the periphery. A scalpel and forceps were used to cut out the block of OCT from the well and replace it in a cryomold. The mold was filled completely with OCT compound and frozen at −80 °C until ready for sectioning. The organoid location within the cryomold was marked to allow for proper orientation when sectioning. The block was sectioned at 10um using a Cryostar nx70.

Immunofluorescence

Slides were allowed to warm up to room temperature. Slides were then placed in distilled water for 1 minute to wash away OCT and then left to dry. A hydrophobic pen was used to draw a hydrophobic circle around each tissue. Tissue was hydrated with PBS + 0.5% Tween (PBS-T) for 20 minutes. The PBS-T was discarded and replaced with a blocking solution consisting of PBS-T 5% BSA, 1/100 Fc Block and 10% serum from species of origin. Slides were incubated with the blocking solution in a humidified chamber for 1 hour. The blocking solution was discarded and replaced with a primary staining solution. Slides were incubated with the primary solution in a humidified chamber overnight at 4C°. The primary staining solution was discarded, and slides were washed 3 times with PBS-T for 5 minutes while shaking gently. The secondary

staining solution was added, and slides were incubated in a humidified chamber for 2 hours. The secondary staining solution was discarded, and the slides were washed 3 times with PBS-T and 1 time with PBS for 5 minutes while shaking gently. 1/3000 DAPI (in PBS) was added onto slides and slides were incubated in a humidified chamber for 3 minutes while shielding from light. DAPI solution was discarded, and slides were washed 3 times with PBS for 5 minutes while shaking gently. Slides were dried slides with kimwipes without disturbing the tissue then air dried. Once tissues/slides were completely dry, a drop of mounting gel for every tissue was placed while avoiding any bubbles. A coverslip was gently placed over the slide and the mounting gel was left to set overnight in the dark.

2D Organoid Generation

Transwells were precoated with 2% (v/v) Matrigel in F12 medium at 37 °C for 1 h. Plates were air-dried for at least 10 min before addition of cells. 3D Organoids were recovered from Matrigel by addition of ice-cold DMEM/F12 medium. Organoids were transferred into a 15 ml tube and centrifuged at 250g for 5 min. Organoid pellets were incubated in TrypLE dissociation medium for 10 min at 37 °C and mechanically suspended by pipetting 20 times. OGM, enhanced with 20% (v/v) FBS (E-OGM) was added to the single cell suspension and centrifuged at 900 ×g for 5 min. Cell pellets were resuspended in E-OGM, counted manually, and added at 100,000 cells/cm2 density in Transwells pre-coated with 2% Matrigel. Confluence was tracked and reached between 3-5 days of incubation at 37 °C (5% CO2).

FITC-Dextran

4 monolayers and controls were prepared on day 0 with 100µl of apical E-OGM and 800 µl of basolateral E-OGM. The controls contained transwells without a monolayer. On day 0, one control and monolayer were apically treated with 100 µL of 1 mg/ml 4 kDa FITC. This was repeated on days 2,3 and 5. At 30, 60, 180 minutes and 24, 48 and 72 hours after treatment, 50 µl of basolateral medium was measured on FITC-dextran contents using fluorescence on a Spectramax M5 with 490 nm excitation and 530 nm emission.

Immunofluorescence Analysis

Immunofluorescent images of gut tissue were analyzed for intensity using the software CellProfiler 4.2.0. The single channel image of the desired antibody was initially converted to greyscale with each pixel assigned an intensity value between 0 and 255 where the former represents the lowest possible intensity value, and the latter represents highest possible intensity. Cell profiler was then used to identify villi in each image using their common characteristics such as average size and shape. Sudden changes in intensity were used to delineate the border of villi. The average intensity per unit area for each villus was then calculated. Representations of the villi identification can be seen in Figure 2 below.

Figure 2

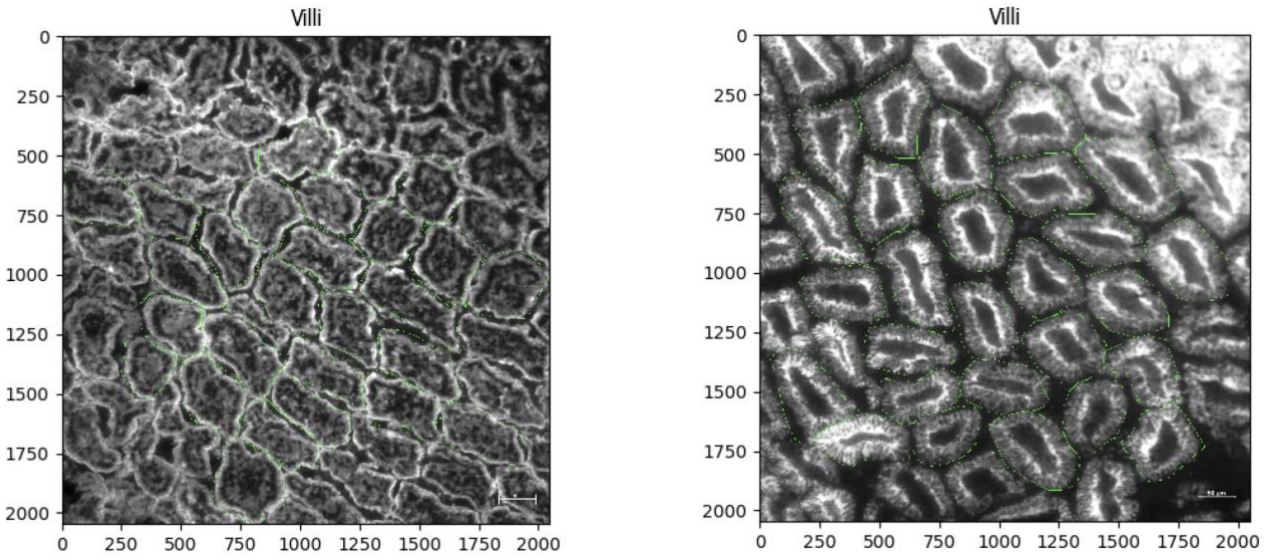

Figure 2: Villi identification using CellProfiler.

Results

E-Cadherin is significantly decreased in Aicda-/- mice by IF

Characterization of the barrier function in WT mouse intestinal tissue was carried out through the immunofluorescent staining and imaging of junction proteins. These include tight junction proteins such as ZO-1 and Occludin as well as adherens junction protein E-Cadherin. These proteins help maintain the polarity of the intestinal epithelium. Figure 3 below represents the immunofluorescent staining of Occludin and E-Cadherin. Occludin staining occurs primarily on the edges of cells on the apical side. E-Cadherin staining occurs along edges of cells as well as between cells.

Figure 3

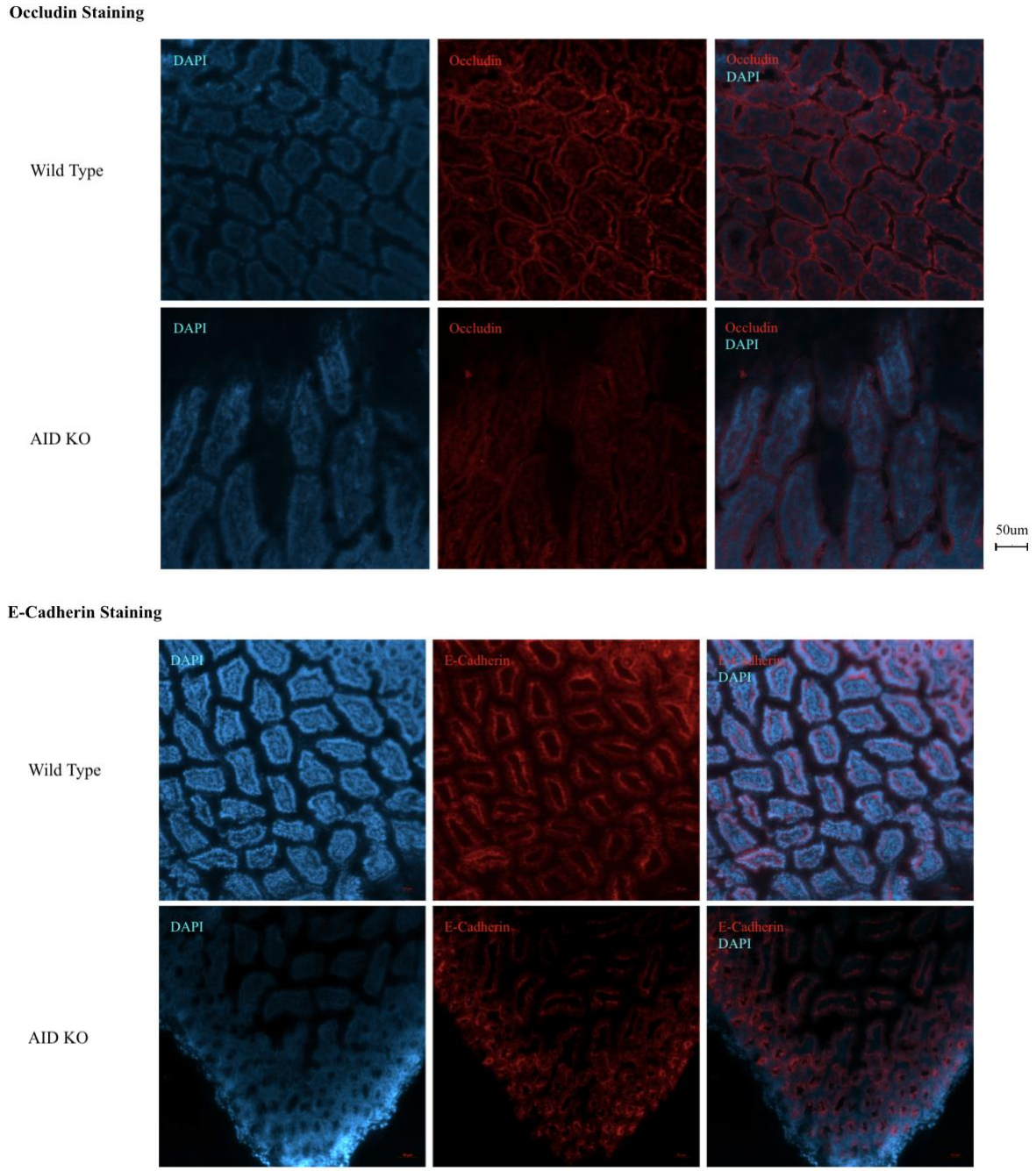

Figure 3: Immunofluorescent staining of WT and AICDA -/- tissue with anti-Occludin and anti-E-cadherin antibodies.

Staining of AID knockout (AICDA -/-) tissue was carried out to characterize the barrier function of the intestinal epithelium in mice lacking the critical immune function of plasma cell generation. This can be observed in Figure 2 above. To quantitatively compare the presence of Occludin and E-Cadherin in the Wild Type (WT) against the AICDA -/-, fluorescent intensity

analysis was carried out on each tissue. All images were taken under identical conditions and tissues were stained simultaneously to control for confounding variables. Figure 4 below compass the fluorescent intensity of WT vs AICDA -/- tissue for both Occludin and E-Cadherin. Here, it can be observed that there is a statistically significant reduction in intensity of villi stained for E-Cadherin between WT and AICDA -/- mouse intestinal tissue. The difference between intensity of villi in WT and AICDA -/- mouse intestinal tissue was not statistically significant for occludin.

Figure 4

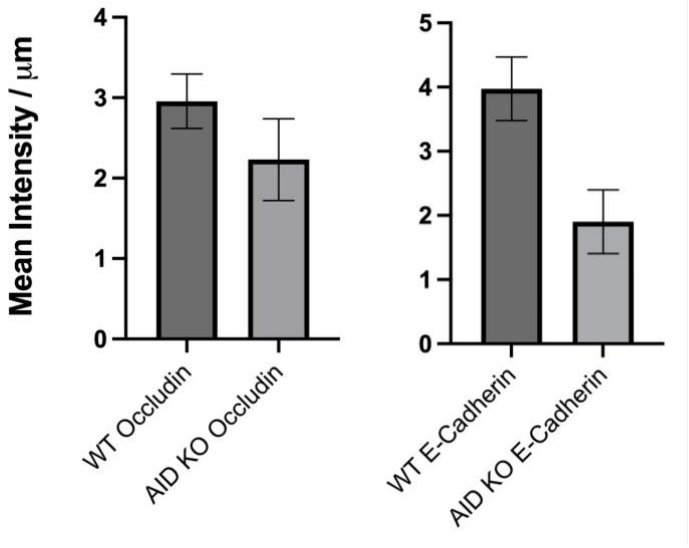

Figure 4: Fluorescence levels of WT vs AICDA -/- mice stained with anti-Occludin (n=1) and anti-E-Cadherin (n=3) antibodies.

No significant changes were observed in Occludin and E-cadherin by RT-PCR
RT-PCR was performed thanks to Resel Periera from the Rojas Lab. Genes associated with the intestinal epithelial junctions were amplified and detected using primers for Occludin and E-Cadherin. This would help capture the genetic expression of these junction markers and provide a quantitative output that would shed light on the comparative gut permeability of the WT vs AICDA -/- mice. Figure 5 below shows the expression of Occludin and E-Cadherin. AICDA -/- mice are equivalent to AICDA -/-. The results show that there was no significant difference between the expression of Occludin or E-Cadherin in WT vs AICDA -/- as can be discerned by RT-PCR.

Figure 5

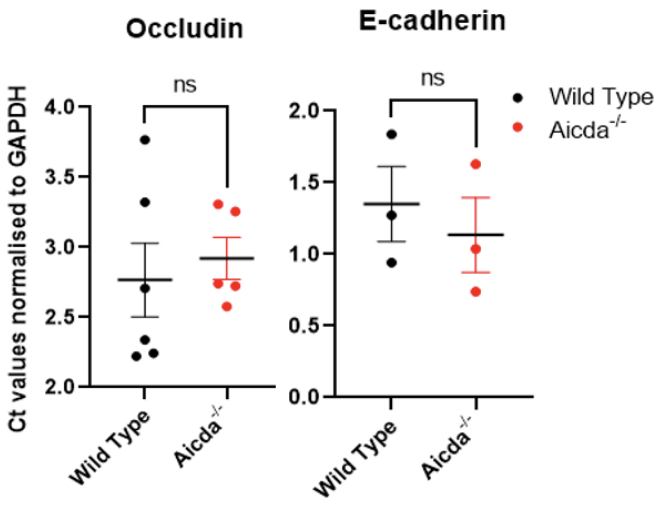

Figure 5: Levels of Occludin and E-Cadherin in WT vs AICDA -/- mouse intestinal tissue as determined by RT-PCR.

An increase of FABP2 measured by ELISA was observed in AICDA -/-

As an additional measure of identifying the presence of increased gut permeability in AICDA -/- mice, a FABP2 ELISA was performed on the serum of WT and AICDA -/- mice (Figure 6). FABP2 is a biomarker for increased gut permeability. Data collection and analysis was done with the help of Resel Periera at the Rojas lab. The concentration of FABP2 in WT mice was significantly lower than the concentration in AICDA -/- mice which indicates an increase in gut permeability.

Figure 6

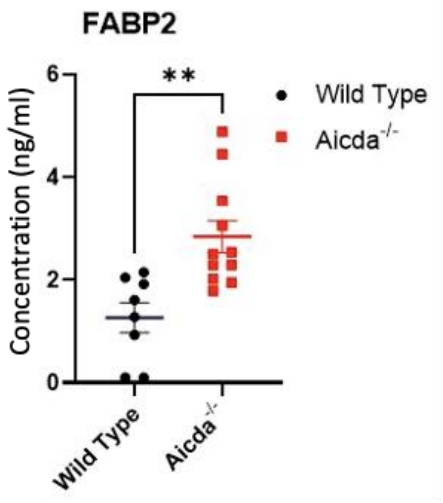

Figure 6: FABP2 levels in the serum of Wild type vs AICDA -/- mice

Generation and IF staining of 3D Mouse Intestinal Organoids from gut derived from WT mice

3D mouse intestinal organoids were grown successfully using the protocol outlined in the methods section. Progression and growth can be seen in Figure 7a below. After initial incubation of crypts, the Organoids began growing villi at approximately day 3. After 6 days of incubation and 2 changes of media, Organoids were ready to be passaged. Dark masses at the centre of the organoids indicate both the production of mucus as well as the deposition of dead cells. Following successful generations of and the preservation of the organoids, immunofluorescence was carried out as a means of characterizing the structure and barrier function of the organoids. This would be critical in evaluating organoids as a suitable model for the gut. Figure 7b below represents the staining of 3D organoids with blue showing DAPI staining and red as a marker for Occludin. Complete rings of cells side by side indicates an ideal organoid structure was generated. DAPI staining at the centre of organoids also indicated the existence of either live cells or DNA from dead cells. Occludin staining in red indicated the existence of continuous tight junctions between the cells of the organoid which mimics the structure observed in WT mouse guts.

Figure 7
a

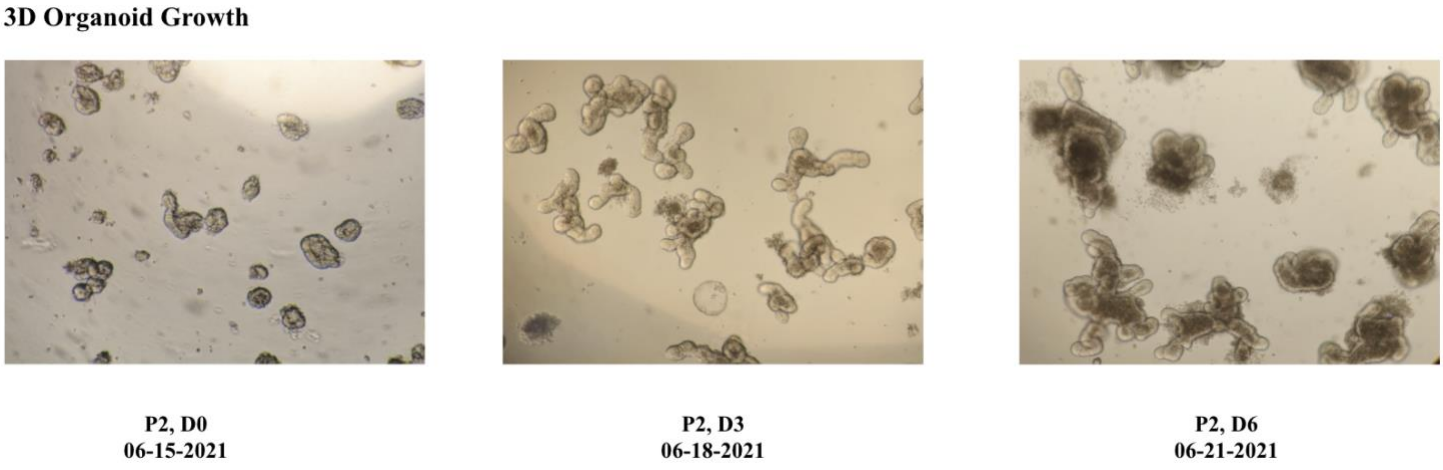

b

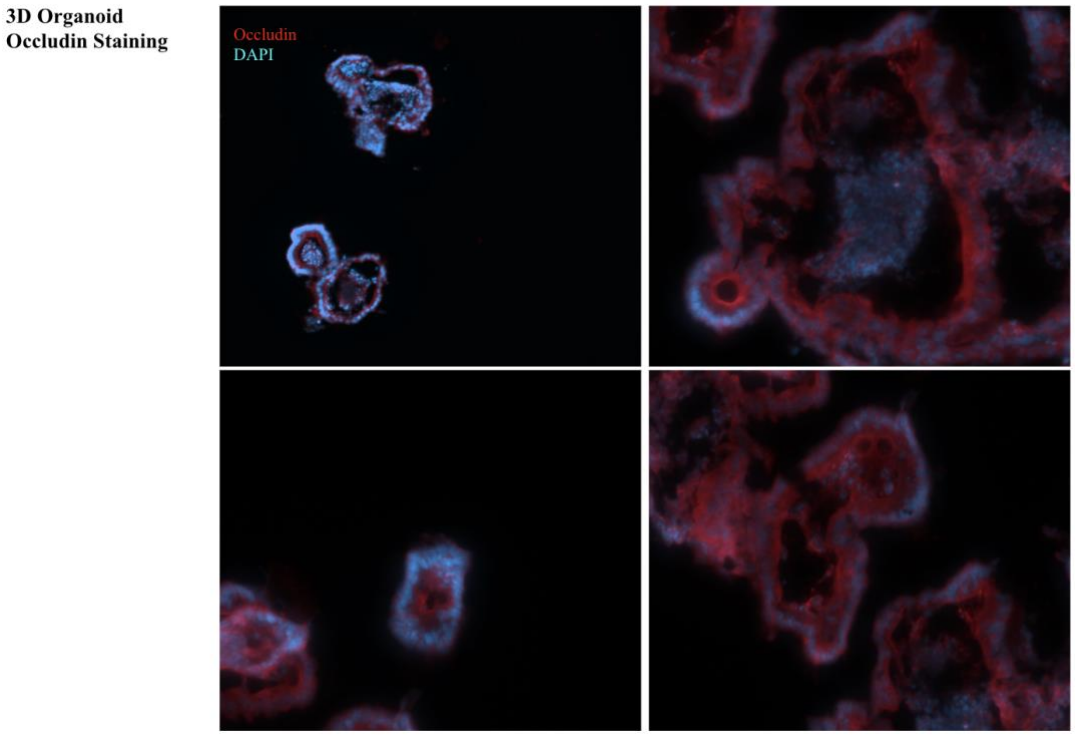

Figure 7: a) Growth of 3D mouse intestinal organoids over a 6-day period. b) Occludin (red) and DAPI (blue) Staining of 3D mouse intestinal organoids sectioned at 10um.

Generation of 2D Monolayer Mouse Intestinal Organoids

Confluent 2D Organoids were successfully generated following the protocol outlined in the methods section. Initial cell seeding of 50k, 100k and 500k cells/well was tested with 100k cells being the most efficient in terms of cell usage and growth. Figure 8a below represents the progression of 2D monolayer growth from Day 0 to confluence at Day 5. Confluence was assessed visually through the identification of gaps throughout the monolayer

Changes in gut epithelial permeability throughout 2D organoids development by FITC-Dextran Permeability Assay

A FITC Dextran permeability assay was carried out as a means of assessing the confluence of 2D monolayer organoids. This would assess whether 2D monolayer organoids could be utilized as a suitable model for gut permeability. The protocol generated and outlined in the methods section would allow for both the verification of confluency of 2D monolayers as well as assess their permeability over a set period. All non-control groups showed statistically significant decrease in fluorescence and therefore permeability in comparison with the control indicating some level of barrier function (Figure 8b). Initial permeability of the day 3 organoid was the lowest by a statistically significant margin indicating the highest actual level of confluence. Despite having the highest level of visual confluency, the day 5 Organoid had the highest-level initial permeability of all non-control groups. This could occur as a result of multiple variables such cell death or barrier deterioration, which is in line with documented rapid deterioration of 2D gut

Monolayers in literature. An increase in fluorescence was observed in all groups as the assay progressed.

Figure 8
a

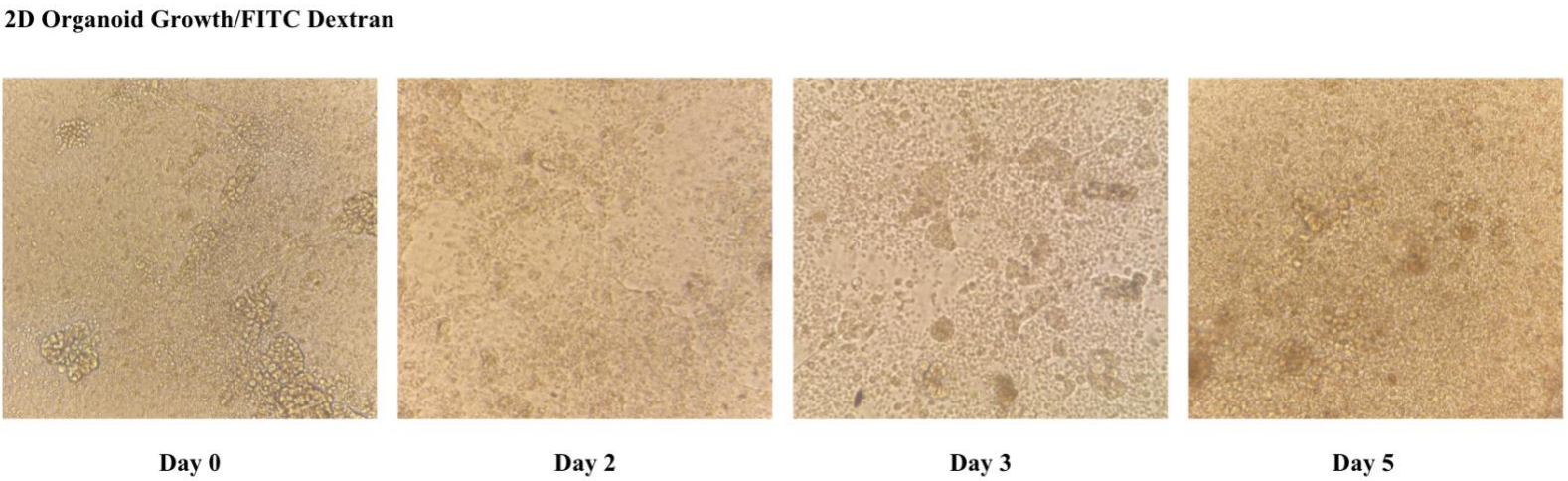

b

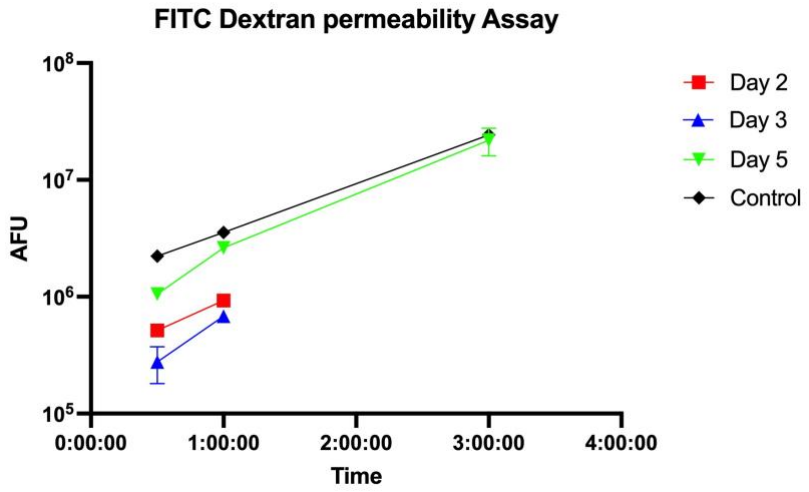

Figure 8: a) Growth of 2D mouse intestinal organoids over a 5-day period. b) FITC-Dextran Permeability assay of 2D mouse intestinal organoids.

Discussion

Through this study, some evidence linking AICDA -/- mice with gut permeability and dysbiosis was established. This was initially carried out using semi-quantitative immunofluorescence analysis of WT and AICDA -/- mouse intestinal tissue for junction markers Occludin and E-Cadherin. These tight and adheren junction markers are responsible for regulating gut permeability and polarity. It was demonstrated that there was a significant decrease in the presence of E-Cadherin in AICDA -/- mice compared to the WT. The change in occludin expression was not significant. This was followed up by RT-PCR which was used to quantify the gene expression of the previously aforementioned markers. This indicated there was no significant difference in the expression of Occludin and E-Cadherin between AICDA -/- and WT mice. Although Occludin and E-cadherin in the gut have been previously studied using immunofluorescence and RT-PCR, reproducing such results would provide a solid foundation for the advancement of this research project.

As a last measure of establishing the initial aim in AICDA -/- mice, an ELISA was carried out for FABP2, a marker of gut permeability, in mouse serum. Results indicated that AICDA -/- mice had a significantly higher level of FABP2 in serum. To further study the mechanisms behind the increase in gut permeability, a 2D/3D mouse intestinal gut organoid was established. Immunofluorescence of the 3D organoids indicated a similar presence of the marker occludin in 3D organoids as observed in WT mouse intestinal tissue. Due to time constraints, immunofluorescent staining of the 2D monolayers could not be optimized and completed. As an alternative validation of the 2D organoids a FITC permeability assay was performed to measure the permeability of generated gut monolayers over time and attempt to pinpoint an ideal timespan for the monolayers to reach confluency. 2D organoids tested on Day 3 displayed the lowest level of gut permeability indicating the highest level of confluence. Across all trials, the movement of FITC across the cell monolayer increased with time.

The project was faced with certain limitations which can be revised. The first of which was the time constraint to carry out the project. Because of the amount of time required for the growth of the organoids, the generation of an expandable organoid line occupied a large proportion of the time needed to carry out the study. This meant that certain research aims could not be reached, such as the testing of various bacterial monocultures, co-cultures and immune cells and their effects on gut permeability in the 2D monolayer organoids. Additionally, the time constraint prevented the optimization of certain methodologies that would have contributed to a more detailed exploration of the primary aims. This included the sectioning and staining of 2D monolayer organoids, which was difficult due to the fragile nature of the monolayers. Alternatively, some experiments such as the FITC-Dextran permeability assay could have been replicated to provide more complete data. The final limitation consisted of sample sizes in certain experiments (ie RT-PCR). Since this project involved working with mice, obtaining a large sample size to boost statistical significance was difficult.

As next steps to follow on from this project, certain experiments must be repeated in order to provide a more accurate date. For experiments that were never optimized, further work needs to be carried out to identify an ideal and practical protocol. Once this is complete, the investigation of the final aim can be executed. Studies of monocultures and cocultures of bacteria on 2D monolayers and how they interface with immune cells can be carried out. This will help identify

phenotypic changes in immune cells brought upon by certain bacteria in the gut and ultimately provide more insight into the mechanisms of how the microbiome can contribute to neurodegeneration and inflammation.

References

1. Rao JN, Wang J-Y. 2010. Intestinal Architecture and Development. Morgan & Claypool Life Sciences.
2. Lueschow SR, McElroy SJ. 2020. The Paneth Cell: The Curator and Defender of the Immature Small Intestine. Frontiers in Immunology. 11:587.
3. Lee B, Moon KM, Kim CY. 2018. Tight Junction in the Intestinal Epithelium: Its Association with Diseases and Regulation by Phytochemicals. J Immunol Res. 2018:2645465.
4. Lee SH. 2015. Intestinal permeability regulation by tight junction: implication on inflammatory bowel diseases. Intest Res. 13(1):11–18.
5. Saitou M, Furuse M, Sasaki H, Schulzke JD, Fromm M, Takano H, Noda T, Tsukita S. 2000. Complex phenotype of mice lacking occludin, a component of tight junction strands. Mol Biol Cell. 11(12):4131–4142.
6. Umeda K, Matsui T, Nakayama M, Furuse K, Sasaki H, Furuse M, Tsukita S. 2004. Establishment and characterization of cultured epithelial cells lacking expression of ZO-1. J Biol Chem. 279(43):44785–44794.
7. Valdes AM, Walter J, Segal E, Spector TD. 2018. Role of the gut microbiota in nutrition and health. BMJ. 361:k2179.
8. Shulzhenko N, Morgun A, Hsiao W, Battle M, Yao M, Gavrilova O, Orandle M, Mayer L, Macpherson AJ, McCoy KD, et al. 2011. Crosstalk between B lymphocytes, microbiota and the intestinal epithelium governs immunity versus metabolism in the gut. Nat Med. 17(12):1585–1593.
9. Glassner KL, Abraham BP, Quigley EMM. 2020. The microbiome and inflammatory bowel disease. J Allergy Clin Immunol. 145(1):16–27.
10. Kho ZY, Lal SK. 2018. The Human Gut Microbiome – A Potential Controller of Wellness and Disease. Frontiers in Microbiology. 9:1835.
11. Zheng D, Liwinski T, Elinav E. 2020. Interaction between microbiota and immunity in health and disease. Cell Res. 30(6):492–506.
12. Zhou J, Zhou Z, Ji P, Ma M, Guo J, Jiang S. 2019. Effect of fecal microbiota transplantation on experimental colitis in mice. Exp Ther Med. 17(4):2581–2586.
13. Morais LH, Schreiber HL, Mazmanian SK. 2021. The gut microbiota–brain axis in behaviour and brain disorders. Nat Rev Microbiol. 19(4):241–255.
14. Jangi S, Gandhi R, Cox LM, Li N, von Glehn F, Yan R, Patel B, Mazzola MA, Liu S, Glanz BL, et al. 2016. Alterations of the human gut microbiome in multiple sclerosis. Nat Commun. 7:12015.
15. Chen J, Chia N, Kalari KR, Yao JZ, Novotna M, Paz Soldan MM, Luckey DH, Marietta EV, Jeraldo PR, Chen X, et al. 2016. Multiple sclerosis patients have a distinct gut microbiota compared to healthy controls. Sci Rep. 6:28484.
16. Cekanaviciute E, Yoo BB, Runia TF, Debelius JW, Singh S, Nelson CA, Kanner R, Bencosme Y, Lee YK, Hauser SL, et al. 2017. Gut bacteria from multiple sclerosis

patients modulate human T cells and exacerbate symptoms in mouse models. PNAS. 114(40):10713–10718.
17. Berer K, Gerdes LA, Cekanaviciute E, Jia X, Xiao L, Xia Z, Liu C, Klotz L, Stauffer U, Baranzini SE, et al. 2017. Gut microbiota from multiple sclerosis patients enables spontaneous autoimmune encephalomyelitis in mice. PNAS. 114(40):10719–10724.
18. Wei M, Shinkura R, Doi Y, Maruya M, Fagarasan S, Honjo T. 2011. Mice carrying a knock-in mutation of Aicda resulting in a defect in somatic hypermutation have impaired gut homeostasis and compromised mucosal defense. Nat Immunol. 12(3):264–270.
19. Fagarasan S, Muramatsu M, Suzuki K, Nagaoka H, Hiai H, Honjo T. 2002. Critical roles of activation-induced cytidine deaminase in the homeostasis of gut flora. Science. 298(5597):1424–1427.
20. Suzuki K, Meek B, Doi Y, Muramatsu M, Chiba T, Honjo T, Fagarasan S. 2004. Aberrant expansion of segmented filamentous bacteria in IgA-deficient gut. PNAS. 101(7):1981–1986.
21. Dutta D, Heo I, Clevers H. 2017. Disease Modeling in Stem Cell-Derived 3D Organoid Systems. Trends Mol Med. 23(5):393–410.
22. Bar-Ephraim YE, Kretzschmar K, Clevers H. 2020. Organoids in immunological research. Nat Rev Immunol. 20(5):279–293.
23. Sato T, Vries RG, Snippert HJ, van de Wetering M, Barker N, Stange DE, van Es JH, Abo A, Kujala P, Peters PJ, et al. 2009. Single Lgr5 stem cells build crypt-villus structures in vitro without a mesenchymal niche. Nature. 459(7244):262–265.
24. Fair KL, Colquhoun J, Hannan NRF. 2018. Intestinal organoids for modelling intestinal development and disease. Philosophical Transactions of the Royal Society B: Biological Sciences. 373(1750):20170217.
25. Nozaki K, Mochizuki W, Matsumoto Y, Matsumoto T, Fukuda M, Mizutani T, Watanabe M, Nakamura T. 2016. Co-culture with intestinal epithelial organoids allows efficient expansion and motility analysis of intraepithelial lymphocytes. J Gastroenterol. 51(3):206–213.
26. Stevens BR, Goel R, Seungbum K, Richards EM, Holbert RC, Pepine CJ, Raizada MK. 2018. Increased human intestinal barrier permeability plasma biomarkers zonulin and FABP2 correlated with plasma LPS and altered gut microbiome in anxiety or depression. Gut. 67(8):1555–1557.
27. Choudhary M, Tamrakar A, Singh AK, Jain M, Jaiswal A, Kodgire P. 2018. AID Biology: A pathological and clinical perspective. Int Rev Immunol. 37(1):37–56.